 doi:10.20944/preprints202102.0282.v1

Article

Triterpenes and phenolic compounds from the fungus *Fuscoporia torulosa*: isolation, structure determination and biological activity

Zoltán Béni [1], Miklós Dékány [1], András Sárközy [2], Annamáris Kincses [3], Gabriella Spengler [3], Viktor Papp [4], Judit Hohmann [2,5*], Attila Ványolós [2,6*]

1 Spectroscopic Research, Gedeon Richter Plc., Gyömrői út 19-21, H-1103 Budapest, Hungary; z.beni@richter.hu, M.Dekany@richter.hu
2 Department of Pharmacognosy, University of Szeged, Eötvös u. 6, H-6720 Szeged, Hungary; sarkozy@pharmacognosy.hu
3 Department of Medical Microbiology and Immunobiology, University of Szeged, Dóm square 10, H-6720, Szeged, Hungary; spengler.gabriella@med.u-szeged.hu, kincses.annamaria@med.u-szeged.hu
4 Department of Botany, Szent István University, H-1118 Budapest, Villányi út 29-43, Hungary; Papp.Viktor@kertk.szie.hu
5 Interdisciplinary Centre for Natural Products, University of Szeged, Eötvös u. 6, H-6720 Szeged, Hungary; hohmann.judit@szte.hu
6 Department of Pharmacognosy, Semmelweis University, Üllői u. 26, H-1085 Budapest, Hungary; vanyolosa@pharmacognosy.hu
*Correspondence: vanyolosa@pharmacognosy.hu; hohmann.judit@szte.hu; Tel.: +36-62-545 558

Abstract: Investigation of the methanol extract of the poroid fungus *Fuscoporia torulosa* resulted in the isolation of a novel triterpene, fuscoporic acid (**1**) together with inoscavin A and its previously undescribed *Z* isomer (**2** and **3**), 3,4-dihydroxy-benzaldehide (**4**), osmundacetone (**5**), senexdiolic acid (**6**), natalic acid (**7**), and ergosta-7,22-diene-3-one (**8**). The structures of fungal compounds were determined on the basis of NMR and MS spectroscopic analysis, as well as molecular modelling studies. Compounds **1**, **6**-**8** were examined for their antibacterial properties on resistant clinical isolates, and cytotoxic activity on human colon adenocarcinoma cell lines. Compound **8** was effective against Colo 205 (IC_{50} 11.65±1.67 μM), Colo 320 (IC_{50} 8.43±1.1 μM) and MRC-5 (IC_{50} 7.92±1.42 μM) cell lines. Potentially synergistic relationship was investigated between **8** and doxorubicin, which revealed a synergism between the examined compounds with a combination index (CI) at the 50% growth inhibition dose (ED_{50}) of 0.521±0.15. Several compounds (**1**, and **6**-**8**) were tested for P-glycoprotein modulatory effect in Colo 320 resistant cancer cells, but none of the compounds proved to be effective in this assay. Fungal metabolites **2**-**5** were evaluated for their antioxidant activity using the oxygen radical absorbance capacity (ORAC) and DPPH assays. Compounds **4** and **5** proved to possess considerable antioxidant effect with EC_{50} 0.25±0.01 (DPPH) and 12.20±0.92 mmol TE/g (ORAC). The current article provides valuable information on both chemical and pharmacological profiles of *Fuscoporia torulosa*, paving the way for future studies with this species.

Keywords: *Fuscoporia torulosa*; triterpenes; cytotoxic; antioxidant; synergism; antibacterial; ORAC; DPPH

1. Introduction

The members of phellinoid Hymenochaetaceae (*Phellinus* s. lato) are considered as an abundant source of diverse bioactive metabolites and the pharmacological potential of wild species are intensely studied all around the world [1–4]. The morphologically circumscribed Phellinus s. lato represents a phylogenetically polyphyletic assemblage that includes smaller and more natural genera [5]. Among these, *Fuscoporia* Murrill is one of the largest genus, distributed on all forested continents [6]. Based on recent taxonomic

Preprints (www.preprints.org) | NOT PEER-REVIEWED | Posted: 11 February 2021 doi:10.20944/preprints202102.0282.v1

studies, 50 species are accepted in the genus, which are divided into six phylogenetic lineages [7,8]. The so called "F. torulosa group" comprises ten species, of which only two have been reported from Europe: *F. wahlbergii* (Fr.) T. Wagner & M. Fisch. and *F. torulosa* (Pers.) T. Wagner & M. Fisch. [7]. The more common *F. torulosa* is widespread in Europe with a preference of southern distribution and grows on various broad-leaved trees or rarely on conifers [9]. The perennial woody basidiocarps of *F. torulosa* develop mainly on the base of living trees, and easily distinguished by its rusty brown color with greenish sterile surface due to the presence of mosses and algae [10].

The first study to explore the chemistry of *F. torulosa* appeared in the mid '90s, which reported the isolation of 9 compounds, among them 3 novel lanosteroids, namely albertic, natalic and torulosic acids [11]. One and a half decades after the first study, Deveci et al. presented the results of an investigation on *F. torulosa* samples of Turkish origin: 1 new and 9 known compounds were isolated. The fungal metabolites were examined for their potential cytotoxic, antioxidant, cholinesterase, and tyrosinase inhibitory activities (Deveci et al.). Besides these mycochemical studies several articles reported on the antimicrobial, antioxidant, cytotoxic and xanthine oxidase inhibitory, and anti-acne activities and the phenolic profile of *F. torulosa* samples prepared with solvents of different polarities [2,12–14].

The present study afforded valuable new information to the chemical profile of *F. torulosa*, and to the pharmacological potential of the isolated fungal metabolites.

2. Results and Discussion

In-depth chemical examination of the methanol extract obtained from fruiting bodies of *F. torulosa* led to the identification of six compounds (**1**-**8**) (Figure 1). The concentrated methanol extract of *F. torulosa* was subjected to solvent-solvent partition between aqueous MeOH and *n*-hexane, followed by extraction with chloroform and ethyl acetate. The obtained organic solvent extracts were separated using a combination of flash column chromatography and reversed-phase HPLC, to give compounds **1**-**8**.

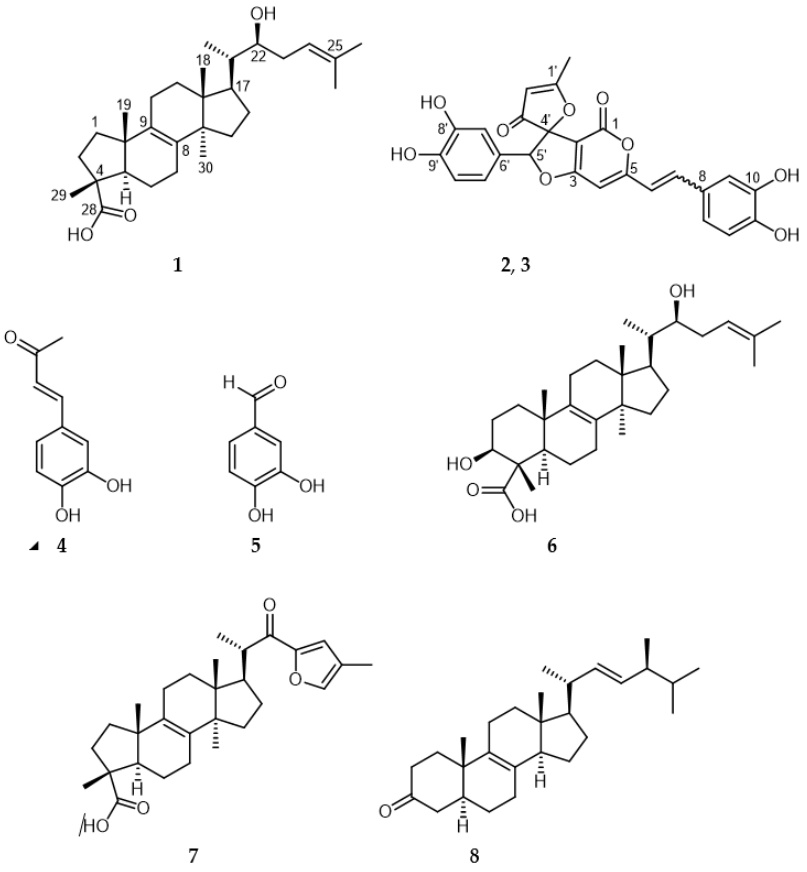

 doi:10.20944/preprints202102.0282.v1

Figure 1. Compounds isolated from *F. torulosa* (**2** and **3** *E*-*Z* isomers)

The ^{1}H and ^{13}C NMR spectra of compound **1** presented similar spectral features to those reported for gilvsin D [15] and obtained for natalic acid (**7**) [16]. Consecutive analysis of the COSY, HSQC and HMBC spectra of **1** showed that it is a structural analogue of gilvsin D and natalic acid (**7**), and enabled the complete ^{1}H and ^{13}C NMR assignments listed in Table 1. Based on the spectral data similarities, all three compounds share the same degraded lanosterol skeleton. Structural differences were found in the side chains attached to C-17. HSQC and HMBC data suggested that in case of compound **1** a 22-hydroxy-24-en side chain was present. 1D and 2D ROESY data were in accordance with the suggested structure and proved that the relative configurations of C-4, C-5, C-10, C-13, C-14, C-17, and C-20 were identical in compound **1** and gilvsin D as well as in natalic acid (**7**). In addition to this, based on the findings of Barrera and coworkers [17] the ca. 3.6 Hz coupling constant observed between H-21 and H-22 suggested an *S* configuration of the C-22 chirality center. Putting these pieces of information together, compound **1** was characterized as 22*S*-hydroxy-8,24-dien-3-norlanosta-28-oic acid, named fuscoporic acid (Figure 1).

Preprints (www.preprints.org) | NOT PEER-REVIEWED | Posted: 11 February 2021 doi:10.20944/preprints202102.0282.v1

Table 1. ^{1}H and ^{13}C NMR assignments of **1**

Position	δ^{13}C ppm	δ^{1}H ppm	Multiplicity (*J* in Hz)
1 α		1.49	m
1 β	36.0	1.60	m
2 α		2.48	dd (13.7, 8.3)
2 β	36.9	1.67	m
4	48.2		
5	52.9	2.06	m
6 α		1.63	m
6 β	18.6	1.72	m
7	25.9	2.12	m
8	134.1		
9	135.0		
10	45.6		
11 α	22.5	2.02	m
11 β		2.13	m
12 α	30.4	1.76	m
12 β		1.69	m
13	45.3		
14	48.9		
15 α	30.6	1.20	m
15 β		1.60	m
16 α	27.3	1.82	m
16 β		1.44	m
17	47.1	1.57	m
18	15.5	0.76	s
19	19.3	0.98	s
20	41.6	1.80	m
21	12.7	0.96	d (6.6)
22	73.4	3.68	m
23	29.1	2.05	m
24	121.3	5.19	m
25	135.2		
26	26.0	1.75	s
27	18.0	1.66	m
28	185.3		
29	21.3	1.24	s
30	24.4	0.89	s

Compounds **2** and **3** represent a mixture of inoscavin A and its *Z* isomer in a ca. 5 to 3 molar ratio. To the best of our knowledge the *cis* isomer has not yet been reported in the literature. Based on the agreement of the obtained and published [18] NMR and HRMS data the major component could be unambiguously assigned as inoscavin A. In accordance with the proposed structure the minor component presented highly similar ^{1}H and ^{13}C NMR features, except those belonging to the hispidine moiety of inoscavin A. Thus, in

Preprints (www.preprints.org) | NOT PEER-REVIEWED | Posted: 11 February 2021 doi:10.20944/preprints202102.0282.v1

the ^{1}H NMR spectrum, instead of the two doublet resonances (δ_H 7.47 and 6.75 ppm) with 15.7 Hz coupling constant, two doublets at δ_H 6.87 and 6.11 ppm with a 12.7 Hz coupling constant were obtained for H-7 and H-6, respectively. These differences were in accordance with the proposition that the double bond between C-6 and C-7 was in *cis* configuration in the minor component. ^{13}C, COSY, HSQC and HMBC data confirmed the proposed structures and enabled the complete ^{1}H and ^{13}C NMR assignments of both components. Homonuclear ROESY data were also in accordance with these structural conclusions.

The relative stereochemistry of the C-4′ and C-5′ stereogenic centers could not be determined on this basis. Although inoscavin A is known for quite some time, no literature data was found that could allow the stereochemical assignment of these centers on a comparative basis either. Unfortunately, the amount of sample did not enable to collect the specific experimental data (e.g. heteronuclear NOE) that might allow to distinguish between the possible diastereoisomers. In the absence of experimental data, a molecular modelling study was undertaken to determine the relative stereochemistry. Using the method described in the Experimental section, NMR shielding constants and chemical shift values were calculated for the (arbitrary chosen) 4′*R*,5′S and 4′*S*,5′*S* epimers (Figure 2) by averaging the appropriate values obtained for four representative conformers using the Boltzmann populations derived from the solution phase energies (SI). As it is shown in Table 2, the resulted unscaled chemical shifts (relative to TMS, using the default Jaguar procedure) are in very good agreement with the experimental data in both cases.

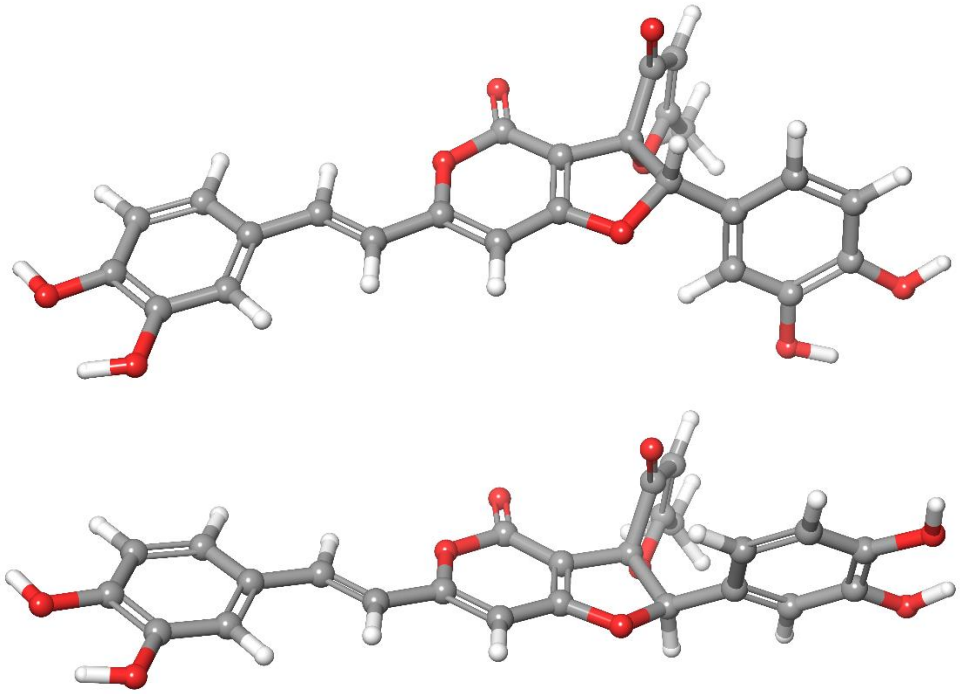

Figure 2. *SS* (top) and *RS* (bottom) epimers of inoscavin A

Preprints (www.preprints.org) | NOT PEER-REVIEWED | Posted: 11 February 2021 doi:10.20944/preprints202102.0282.v1

Table 2. Experimental and calculated chemical shifts and isotropic shielding values of *S,S* and *R,S* isomers

No.	Atom No in Figure 1	δ_{exp} Experimental shift (ppm)	*SS* Boltzmann averaged shielding	*RS* Boltzmann averaged shielding	δcalc *SS* unscaled shift (ppm) *	δs *SS* scaled shift (ppm)	δcalc *RS* unscaled shift (ppm) *	δs *RS* scaled shift (ppm)
C1	**Me**	**16.8**	165.1	164.5	16.2	16.3	16.8	16.3
C2	**1'**	**193.1**	-18.1	-18.5	195.1	195.1	195.5	195.8
C3	**2'**	**105.3**	74.1	74.8	105.1	105.2	104.4	104.3
C4	**3'**	**203.3**	-25.1	-24.1	202.0	202.0	201.0	201.3
C6	**4'**	**94.4**	82.5	80.5	96.9	97.0	98.8	98.7
C8	**5'**	**96.0**	83.0	85.5	96.4	96.5	93.9	93.7
C10	**3**	**177.0**	0.6	0.8	176.9	176.9	176.6	176.9
C11	**2**	**99.6**	80.7	79.5	98.6	98.7	99.8	99.7
C12	**1**	**160.8**	19.3	18.9	158.6	158.7	159.0	159.1
C15	**5**	**167.2**	9.0	9.2	168.6	168.7	168.4	168.6
C16	**4**	**95.7**	84.1	83.8	95.3	95.4	95.6	95.4
C17	**6**	**116.8**	62.3	62.5	116.6	116.6	116.4	116.4
C18	**7**	**140.7**	36.6	36.8	141.7	141.8	141.5	141.6
C19	**8**	**128.6**	48.5	48.8	130.0	130.1	129.8	129.8
C20	**9**	**115.2**	64.5	64.3	114.4	114.5	114.7	114.6
C21	**10**	**147.1**	31.2	31.2	146.9	147.0	147.0	147.0
C22	**11**	**149.6**	30.3	30.4	147.9	147.9	147.7	147.8
C23	**12**	**116.1**	63.7	63.7	115.3	115.3	115.2	115.2
C24	**13**	**122.8**	54.3	54.5	124.4	124.5	124.2	124.2
C27	**6'**	**123.3**	52.1	51.4	126.6	126.7	127.2	127.2
C28	**7'**	**115.6**	64.0	62.9	114.9	115.0	116.0	115.9
C29	**8'**	**146.4**	31.6	32.0	146.6	146.7	146.2	146.3
C30	**9'**	**148.0**	31.9	32.1	146.3	146.4	146.1	146.2
C31	**10'**	**116.8**	65.2	65.3	113.8	113.9	113.7	113.6
C32	**11'**	**120.4**	59.2	57.8	119.6	119.7	121.0	121.0
H35	**5'**	**5.68**	26.27	25.92	5.56	5.51	5.90	5.75
H36	**6**	**6.75**	24.88	24.98	6.90	6.80	6.80	6.67
H37	**7**	**7.47**	23.99	23.93	7.75	7.61	7.80	7.71
	Me	**2.00**	29.95	29.54	2.03	2.13	2.43	2.20
H41	**2'**	**5.60**	26.33	26.65	5.51	5.46	5.20	5.03
H42	**4**	**6.53**	25.53	25.64	6.27	6.19	6.17	6.03
H43	**9**	**7.10**	24.30	24.31	7.45	7.32	7.44	7.33
H44	**12**	**6.78**	24.87	24.86	6.90	6.80	6.92	6.80
H45	**13**	**7.02**	24.54	24.54	7.22	7.10	7.22	7.11
H48	**7'**	**6.73**	24.83	24.67	6.94	6.84	7.10	6.99
H49	**10'**	**6.82**	24.94	24.94	6.84	6.74	6.84	6.72
H50	**11'**	**6.61**	25.08	24.88	6.70	6.61	6.89	6.77

Preprints (www.preprints.org) | NOT PEER-REVIEWED | Posted: 11 February 2021 doi:10.20944/preprints202102.0282.v1

* δ_{calc} unscaled shift are calculated by Jaguar relative to TMS (based on a semi empirical linear regression against experimental data); δ_s scaled shifts are calculated according to $\delta_s = (\delta_{calc} - b)/m$, where b and m are the intercept and slope of a plot of δ_{calc} against δ_{exp}

The mean absolute error (MAE) calculated for $^{13}C/^{1}H$ chemical shifts were 1.2 /0.17 ppm in the case of the *SS* and 1.3/0.26 ppm for the *RS* epimer, respectively. The scaled shifts [19,20] agreed even better with the experimental values by showing (corrected) MAE values of $^{13}C/^{1}H$ 1.2/0.12 and 1.3/0.21 ppm for the *SS** and *RS** isomers, respectively. Although only small differences were obtained, these were consistently pointing towards the presence of the *SS** isomer. Recently Grimblat et al. [21] showed that the extended and combined use of DP4 probability function introduced by Smith et al. [22] could successfully help to solve structural questions where other methods failed. Applying their DP4+ methodology on the calculated isotropic shielding values (shielding are listed in Table 2, DP4+ probabilities calculated by the template provided by the authors, are shown in Table 3), in our case the *SS* isomer was predicted as the most probable (with a 100% overall possibility) structural candidate. Based on these results compound **2** is described as the mixture of C-4'*S**, C-5'*S** inoscavin A and its *cis* analogue. Considering the obtained optical rotation value of $[\alpha]_D^{25} = 0$ (*c*, 0.05, MeOH), the sample is a racemate.

Table 3. DP4+ probabilities obtained for *SS* and *RS* isomers of **2** and **3** using the template from [21], s and u are referring for scaled and unscaled shifts

	SS	*RS*
sDP4+ (H data)	99.87%	0.13%
sDP4+ (C data)	96.73%	4.27%
sDP4+ (all data)	100%	0%
uDP4+ (H data)	100%	0%
uDP4+ (C data)	79.89%	20.11%
uDP4+ (all data)	100%	0%
DP4+ (H data)	100%	0%
DP4+ (C data)	99.16%	0.84%
DP4+ (all data)	100%	0%

Compounds **4**-**8** reported here were structurally characterized on the basis of HRMS, and standard one- and two-dimensional NMR data in comparison to those reported in the literature. According to spectral analysis **4** and **5** represent an equimolar mixture of 3,4-dihydroxy-benzaldehide and osmundacetone. The remaining constituents are triterpenes, namely senexdiolic acid (**6**), natalic acid (**7**), and ergosta-7,22-diene-3-one (**8**).

The identified fungal constituents were subjected to different pharmacological assays to determine their characteristic biological activities. In this way cytotoxic effect of **1**, **6**-**8** was tested on sensitive and resistant Colo 205 and Colo 320 cell lines, respectively, and on normal MRC-5 embryonal fibroblast cell line along with doxorubicin as a standard. While compounds **1**, **6** and **7** did not show any significant effect in the applied concentration, **8** was effective against both Colo 205 (IC_{50} 11.65±1.67 μM), Colo 320 (IC_{50} 8.43±1.1 μM) and MRC-5 (IC_{50} 7.92±1.42 μM) cell lines. These results proven to be comparable to those of doxorubicin (IC_{50} 2.46±0.26 μM, 7.44±0.2 μM and >20 μM, respectively). After the promising results, a potentially synergistic relationship was investigated between **8** and doxorubicin. For this end a checkerboard combination assay was utilized using resistant Colo 320 cell line as test subject. The results indicated, that 11.2:1 compound **8** : doxorubicin ratio was ideal. At this rate, the Combination Index (CI) at the 50% growth inhibition dose (ED_{50}) was 0.521±0.15, indicating a synergism between the examined compounds. The ef-

Preprints (www.preprints.org) | NOT PEER-REVIEWED | Posted: 11 February 2021 doi:10.20944/preprints202102.0282.v1

fect of compounds **1**, and **6**-**8** on modulation of P-gp efflux was evaluated by flow cytometry, measuring the rhodamine-123 accumulation in MDR Colo 320 human colon adenocarcinoma cells. Tariquidar (0.2 μM), a well-known P-gp inhibitor was used as positive control. The compounds were tested at 2 and 20 μM: P-gp modulating effect was obtained at 2 μM concentrations with compound **8**, at 20 μM in case of compounds **1**, **6**, **7**. The FAR values were used to assess the P-gp modulating potential. Usually, compounds can be considered to be active when presenting FAR values higher than 2. The results presented in Table 4 show that FAR values are in the range of 0.828-1.139, therefore the tested compounds are not effective modulators on drug resistant strain Colo 320.

Table 4. Effect of compounds **1**, **6**-**8** on the P-glycoprotein (P-gp) mediated rhodamine-123 efflux on MDR human colon adenocarcinoma (Colo 320)

Samples	conc. (μM)	FSC	SSC	FL-1	FAR
Tariquidar	0.2	1945	837	64.100	5.533
1	20	2005	851	13.200	1.139
6	20	2074	861	11.900	1.027
7	20	2095	891	12.200	1.053
8	2	2099	857	10.100	0.872
DMSO	2.00%	2073	848	9.590	0.828
Colo 320	-	2052	841	8.870	-

Parameters evaluated from flow cytometric experiments were: Forward Scatter Count (FSC, provides information about cell size); Side Scatter Count (SSC, proportional to cell granularity or internal complexity); FL-1 (Mean fluorescence of the cells) and Fluorescence Activity Ratio (FAR), which was calculated by the equation given in the Materials and Methods.

The antimicrobial effect of compounds **1**, and **5-7** were determined on *Escherichia coli* ATCC 25922, *Salmonella enterica* serovar Typhimurium 14028s, *Staphylococcus aureus* ATCC 25923 and *S. aureus* 27213 (methicillin and ofloxacin resistant clinical isolate) strains, however none of the compounds produced significant antibacterial effect.

The antioxidant capacity of compounds **2**+**3** and **4**+**5** was determined by DPPH and ORAC assays. While both of the examined samples exhibited antioxidant effects in the two *in vitro* tests, **4**+**5** produced more promising results with 0.25±0.01 μg/mL EC_{50} (DPPH) and 12.20±0.92 mmol TE/g (ORAC), comparable to that of the reference compound, ascorbic acid (Table 5).

Table 5. Antioxidant activity of compounds **2**-**5**.

Compounds	DPPH EC_{50} (μg/mL)	ORAC Activity (mmol TE/g)
2+**3**	0.72±0.05	2.70±0.03
4+**5**	0.25±0.01	12.20±0.92
Ascorbic acid	0.89±0.02	6.94 ± 0.58

3. Materials and Methods

Optical rotations were measured with a Perkin-Elmer 341 polarimeter. The chemicals used in the experiments were supplied by Sigma-Aldrich Hungary and Molar Chemicals, Hungary. Flash chromatography was carried out on a CombiFlash®Rf+Lumen instrument with integrated UV, UV-VIS and ELS detection using RediSep Rf Gold Normal Phase Silica Flash columns (4, 12 and 60 g) (Teledyne Isco, Lincoln, USA). Reversed-phase

 doi:10.20944/preprints202102.0282.v1

HPLC (RP-HPLC) separations were performed on a Wufeng LC-100 Plus HPLC instrument equipped with a UV-VIS detector (Shanghai Wufeng Scientific Instruments Co., Ltd., Shanghai, China) at 254 nm, using a Zorbax ODS column (250 × 4 mm, 5 μm; Agilent Technologies, Santa Clara, CA, USA).

HRMS and MS analyses were performed on a Thermo Velos Pro Orbitrap Elite and Thermo LTQ XL (Thermo Fisher Scientific) system. The ionization method was ESI operated in positive (or negative) ion mode. The (de)protonated molecular ion peaks were fragmented by CID at a normalized collision energy of 35%. For the CID experiment helium was used as the collision gas. The samples were dissolved in methanol. Data acquisition and analysis were accomplished with Xcalibur software version 4.0 (Thermo Fisher Scientific). NMR data were acquired on a Bruker Avance III HD 800 or 500 MHz NMR spectrometer (Bruker, Rheinstetten, Germany) both equipped with a TCI cold probe. MeOD-d_4 or $CDCl_3$ were used as solvents. Chemical shifts are reported in the delta scale relative to the residual solvent signals (3.31/7.27 and 49.15/77.0 ppm for ^{1}H and ^{13}C in MeOD/$CDCl_3$, respectively). Standard one- and two-dimensional NMR spectra were recorded in all cases, using the pulse sequences available in the TopSpin 3.5 sequence library. Data analysis and interpretation were performed with ACD/Labs 2017.1.3 NMR Workbook Suite.

Molecular modelling study was performed within the Jaguar software package (Jaguar, version 10.4, Schrodinger, Inc., New York, NY, 2019.) [23]**.** Firstly, a conformational search was performed at the MM level using the default settings in MacroModel. After manual inspection of the resulted conformers four representative conformers of each diastereomers were chosen for QM level geometry optimization using the Jaguar software package (Jaguar, version 10.4, Schrodinger, Inc., New York, NY, 2019.)[23] The gas phase geometry optimizations were performed at the B3LYP-D3/6-31+G** level while NMR shielding constants were calculated on the resulted geometries using B3LYP functional and 6-311+G** basis set and PCM solvent model of methanol. The resulted isotropic shielding values of the conformers were Boltzmann averaged based on the calculated solution phase energies. Finally, DP4+ statistical analysis of these shieldings (with respect to the experimental chemical shifts) was carried out following the method - and applying the template published by Grimblat, Zanardi and Sarotti [21].

3.1. Mushroom material

The mushroom samples were collected in March 2017 from Mt. Gerecse in Central Transdanubia region, Hungary and in April 2018 from the Botanical Garden of Buda. The former sample was found on Austrian oak, black locust and small-leaved linden trees, the latter however was harvested from black locust unanimously. A voucher specimen have been deposited in the mycological collection of Viktor Papp (PV1172).

3.2. Extraction and isolation

The air-dried mushroom material (1.4 kg) was ground, then extracted with MeOH (20 L) at room temperature. After concentration, the MeOH extract (44.26 g) was dissolved in 50% aqueous MeOH and subjected to solvent-solvent partition with *n*-hexane (5 × 300 mL), chloroform (6 × 300 mL) and ethyl acetate (6 × 300 mL). The *n*-hexane fraction (10.34 g) was subjected to flash chromatography on a silica gel column using a gradient system of *n*-hexane and acetone (0–40%; *t* = 55 min). Fractions with similar compositions were combined according to TLC monitoring (A1-A10). The combined fractions A2 and A3 (0.80 g) were purified by flash chromatography using a mixture of *n*-hexane and acetone (0–25%; *t* = 50 min), with increasing polarity, to obtain compounds **7** (2.9 mg). Fractions A4 and A5 (4.99 g) were further separated by multiple flash chromatography steps, applying *n*-hexane–acetone and H_2O-MeOH solvent systems on normal and reversed phase stationary phases, respectively, then a final purification was performed by RP-HPLC using a H_2O-MeOH gradient system to give compounds **1** (14.4 mg) and **6** (9.6 mg).

The chloroform soluble phase (13.47 g) was subjected to flash chromatography in multiple steps on silica gel column using gradient system of *n*-hexane–acetone. Fractions

Preprints (www.preprints.org) | NOT PEER-REVIEWED | Posted: 11 February 2021 doi:10.20944/preprints202102.0282.v1

with similar compositions were combined according to TLC monitoring (B1-B13). Fractions B6-B8 (2.16 g) were further separated by combination of flash chromatography (*n*-hexane–acetone 5% to 25%, *t* = 50 min) to obtain an equimolar mixture of **3** and **4** (62.3 mg) and **5** (4.7 mg).

Finally, the ethyl acetate phase (10.60 g) was further separated in subsequent flash chromatography steps, then fractions with related compositions were combined according to TLC monitoring (B1-B9). The fractionation of C2-4 (0.62 g) by normal phase flash chromatography using a chloroform–MeOH system (0-40%, *t* = 50 min) led to the isolation of **2** (1.4 mg).

Fuscoporic acid (**1**): white, amorphous solid; α_D^{25}+28 (MeOH, *c* 0.1),^{1}H and ^{13}C-NMR data see in Table 1; HRMS: [M-H]$^-$ 441.33698 (delta=-1.0 ppm; $C_{29}H_{45}O_3$). HR-ESI-MS-MS (CID=45%; rel. int. %): 411(36); 371(100).

3.3. Cell culture

The human colon adenocarcinoma cell lines, the Colo 205 (ATCC-CCL-222) doxorubicin-sensitive parent and Colo 320/MDR-LRP (ATCC-CCL-220.1) resistant to anticancer agents expressing ABCB1, were purchased from LGC Promochem (Teddington, UK). The cells were cultured in RPMI-1640 medium supplemented with 10% heat-inactivated fetal bovine serum (FBS), 2 mM L-glutamine, 1 mM Na-pyruvate, 100 mM Hepes, nystatin and a penicillin-streptomycin mixture in concentrations of 100 U/L and 10 mg/L, respectively. The MRC-5 (ATCC CCL-171) human embryonic lung fibroblast cell line (LGC Promochem) was cultured in EMEM medium, supplemented with 1% non-essential amino acid (NEAA) mixture, 10% heat-inactivated FBS, 2 mM L-glutamine, 1 mM Na-pyruvate, nystatin, and a penicillin-streptomycin mixture in concentrations of 100 U/L and 10 mg/L, respectively. The cell lines were incubated in a humidified atmosphere (5% CO_2, 95% air) at 37 ºC.

3.4. Assay for cytotoxic effect

The effects of increasing concentrations of the compounds on cell growth were tested in 96-well flat-bottomed microtiter plates. The two-fold serial dilutions of the tested compounds were made starting with 100 μM. Then, 10^4 of human colonic adenocarcinoma cells in 100 μL of the medium (RPMI-1640) were added to each well, except for the medium control wells. The adherent human embryonic lung fibroblast cell line (10^4/well) was seeded in EMEM medium in 96-well flat-bottomed microtiter plates for 4 hours before the assay. The serial dilutions of the compounds were made in a separate plate starting with 100 μM, and then transferred to the plates containing the adherent corresponding cell line. Culture plates were incubated at 37 °C for 24 h; at the end of the incubation period, 20 μL of MTT (thiazolyl blue tetrazolium bromide) solution (from a 5 mg/mL stock solution) were added to each well. After incubation at 37 °C for 4 h, 100 μL of sodium dodecyl sulfate (SDS) solution (10% SDS in 0.01 M HCl) were added to each well and the plates were further incubated at 37 °C overnight. Cell growth was determined by measuring the optical density (OD) at 540 nm (ref. 630 nm) with Multiscan EX ELISA reader (Thermo Labsystems, Cheshire, WA, USA). Inhibition of cell growth was expressed as IC_{50} values, defined as the inhibitory dose that reduces the growth of the cells exposed to the tested compounds by 50%. IC_{50} values and the SD of triplicate experiments were calculated by using GraphPad Prism software version 5.00 for Windows with nonlinear regression curve fit (GraphPad Software, San Diego, CA, USA; www.graphpad.com).

3.5. Checkerboard combination assay

A checkerboard microplate method was applied to study the effect of drug interactions between the compound **8** and the chemotherapeutic drug doxorubicin. The assay was carried out on Colo 320 colon adenocarcinoma cell line. The final concentration of the compounds and doxorubicin used in the combination experiment was chosen in accordance with their cytotoxicity towards this cell line. The dilutions of doxorubicin were made in a horizontal direction in 100 μL, and the dilutions of the compounds vertically in the microtiter plate in 50 μL volume. Then, 6×10^3 of Colo 320 cells in 50 μL of the medium

Preprints (www.preprints.org) | NOT PEER-REVIEWED | Posted: 11 February 2021 doi:10.20944/preprints202102.0282.v1

were added to each well, except for the medium control wells. The plates were incubated for 72 h at 37 °C in 5% CO_2 atmosphere. The cell growth rate was determined after MTT staining. At the end of the incubation period, 20 µL of MTT solution (from a stock solution of 5 mg/ml) were added to each well. After incubation at 37 °C for 4 h, 100 µL of SDS solution (10% in 0.01 M HCI) were added to each well and the plates were further incubated at 37 °C overnight. OD was measured at 540 nm (ref. 630 nm) with Multiscan EX ELISA reader. Combination index (CI) values at 50% of the growth inhibition dose (ED_{50}) were determined using CompuSyn software (ComboSyn, Inc., Paramus, NJ, USA) to plot four to five data points at each ratio. CI values were calculated by means of the median-effect equation, according to the Chou–Talalay method, where CI<1, CI=1, and CI>1 represent synergism, additive effect (or no interaction), and antagonism, respectively [24,25].

3.6. Rhodamine 123 accumulation assay

The cell numbers of the human colon adenocarcinoma cell lines were adjusted to 2×10^6 cells/mL, re-suspended in serum-free RPMI 1640 medium and distributed in 0.5 mL aliquots into Eppendorf centrifuge tubes. The tested compounds were added at 2 or 20 µM concentrations, and the samples were incubated for 10 min at room temperature. Tariquidar was applied as positive control at 0.2 µM. DMSO at 2% v/v was used as solvent control. Next, 10 µL (5.2 µM final concentration) of the fluorochrome and ABCB1 substrate rhodamine 123 (Sigma) were added to the samples and the cells were incubated for a further 20 min at 37 ºC, washed twice and re-suspended in 1 mL PBS for analysis. The fluorescence of the cell population was measured with a PartecCyFlow® flow cytometer (Partec, Münster, Germany). The fluorescence activity ratio was calculated as the quotient between FL-1 of treated/untreated resistant Colo 320 cell line over treated/untreated sensitive Colo 205 cell line according to the following equation:

$$FAR = \frac{Colo320_{treated} / Colo320_{control}}{Colo205_{treated} / Colo205_{control}}$$

3.7. Bacterial strains

Escherichia coli ATCC (American Type Culture Collection) 25922, *Salmonella enterica* serovar Typhimurium 14028s, *Staphylococcus aureus* ATCC 25923 and the methicillin and ofloxacin resistant *S. aureus* 272123 clinical isolates were used in the study.

3.8. Determination of minimum inhibitory concentrations by microdilution method

The minimum inhibitory concentrations (MICs) of all tested compounds were determined according to the Clinical and Laboratory Standards Institute (CLSI) guidelines in three independent assays. The compounds were diluted in 100 µL of Mueller-Hinton medium in 96-well flat-bottomed microtiter plates. 10^{-4} dilution of an overnight bacterial culture in 100 µL of medium were then added to each well, with the exception of the medium control wells. The plates were further incubated at 37 ºC for 18 h; at the end of the incubation period, were determined MIC values of tested compounds by naked eyes.

3.9. DPPH assay

A method based on the description of Miser-Salihoglu E. et al. was applied [26]. The examination was performed on a FLUOstar Optima BMG Labtech plate-reader with 96-well microplates. The samples were measured in a DMSO environment with the volume of 150 µL per sample resulting 1 mg/mL concentration. Every well contained 50 µL (100 µM) of this base solution for the absorbance measurement (30 min., 550 nm). In case of samples showing no or minor activity, the concentration was doubled for a follow up measurement. In case of the most active samples half maximal effective concentration (EC_{50}) was also determined using a dilution series beginning with 100 µM solution and

 doi:10.20944/preprints202102.0282.v1

halve it in every consecutive step. For data evaluation GraphPad Prism 6.0 software was utilized. The DPPH (2,2′-diphenyl-1-picrylhydrazyl) reagent necessary for the process was supplied by from Sigma-Aldrich Hungary.

3.10. ORAC assay

A method based on the description of Mielnik et al. was applied [27]. 20 µL of the samples were used in 0.01 mg/mL concentration with a 96-well black microplate. In each well 60 µL of AAPH (12 mM final concentration) and 120 µL of fluorescein solution (70 nM final concentration) was added. The fluorescence alteration of each sample was measured for 3 hours with 1.5 min cycle intervals by a FLUOstar Optima BMG Labtech plate-reader. Trolox ((±)-6-hydroxy-2,5,7,8-tetramethyl-chromane-2-carboxylic acid) was used as a standard. Both Trolox and AAPH was supplied by Sigma-Aldrich Hungary, while Fluorescein was provided by Fluka analytical, Japan. For data analysis GraphPad Prism 6.0 software was used. The results were expressed as mmol Trolox equivalent per g of dry material (mmloTE/g).

4. Conclusions

The present report highlights the most important results acquired upon a detailed chemical analysis of *Fuscoporia torulosa* and a valuable addition to further biological activity studies of this species. The combination of chromatographic methods led to the identification of 6 compounds including the novel fuscoporic acid (**1**) and Z- inoscavin A. Biological activity (cytotoxicity, synergictic, MDR reversal, antioxidant and antibacterial) assays were performed to explore the pharmacological potential of chemical constituents of this fungus. The results obtained revealed that ergosta-7,22-diene-3-one (**8**) not only possess considerable cytotoxic effect on human colon adenocarcinoma cell lines, but also exhibits synergism with the reference compound doxorubicin**.** In summary this study provides notable evidence for the increased interest for the polypore *F. torulosa* as a source of fungal metabolites with antioxidant and cytotoxic properties.

Supplementary Materials: 1D, 2D NMR and MS data of the isolated compounds and calculated NMR shielding constants and chemical shift values are available online at www.mdpi.com/xxx/s1.

Author Contributions: A.S. performed the extraction, isolation, and the antioxidant assays; Z.B. and M.D. performed the spectral analysis and structure determination; V.P. provided sample collection and identification, J.H. and A.V. conceived and designed the experiments; A.K. and G.S. performed the cytotoxicity, checkerboard combination and rhodamine accumulation assays and assay for antibacterial activity; Z.B., V.P. and A.V. wrote the paper. All authors have read and agreed to the published version of the manuscript.

Funding: Financial support for this research were provided by the Economic Development and Innovation Operative Program GINOP-2.3.2-15-2016-00012, and the National Research, Development and Innovation Office, Hungary (NKFIH; K135845).

Conflicts of Interest: The authors declare no conflict of interest.

Sample Availability: Samples of the compounds **1, 3**-**7** are available from the authors.

References

1. Dai, Y.-C. Hymenochaetaceae (Basidiomycota) in China. *Fungal Divers.* **2010**, *45*, 131–343.
2. Kovacs, B.; Zomborszki, Z.P.; Orban-Gyapai, O.; Csupor-Loffler, B.; Liktor-Busa, E.; Lazar, A.; Papp, V.; Urban, E.; Hohmann, J.; Vanyolos, A. Investigation of antimicrobial, antioxidant, and xanthine oxidase-inhibitory activities of Phellinus (Agaricomycetes) mushroom species native to Central Europe. *Int. J. Med. Mushrooms* **2017**, *19*, 387–394.
3. Deshmukh, S.; Prakash, V.; Gupta, M. *Advances in Macrofungi*; Sridhar, K.R., Deshmukh, S.K., Eds.; CRC Press: Boca Raton, FL, 2019; pp. 277-303.

4. Sárközy, A.; Kúsz, N.; Zomborszki, Z.P.; Csorba, A.; Papp, V.; Hohmann, J.; Vanyolos, A. Isolation and characterization of chemical constituents from the poroid medicinal mushroom *Porodaedalea chrysoloma* (Agaricomycetes) and their antioxidant activity. *Int. J. Med. Mushrooms* **2020**, *22*, 125–131.
5. Dai, Y.-C.; Zhou, L.-W.; Cui, B.-K.; Chen, Y.-Q.; Decock, C. Current advances in Phellinus sensu lato: medicinal species, functions, metabolites and mechanisms. *Appl. Microbiol. Biotechno.l* **2010**, *87*, 1587–1593.
6. He, M.-Q.; Zhao, R.-L.; Hyde, K.D.; Begerow, D.; Kemler, M.; Yurkov, A.; McKenzie, E.H.C.; Raspé, O.; Kakishima, M.; Sánchez-Ramírez, S.; et al. Notes, outline and divergence times of Basidiomycota. *Fungal Divers.* **2019**, *99*, 105–367.
7. Chen, Q. Global diversity and phylogeny of Fuscoporia (Hymenochaetales, Basidiomycota). *Mycosphere* **2020**, *11*, 1477–1513.
8. Du, P.; Chen, Q.; Vlasák, J. *Fuscoporia ambigua* Sp. Nov., a new species from America and China. *Phytotaxa* **2020**, *456*, 175–185.
9. Ryvarden, L.; Melo, I. *Poroid Fungi of Europe*; Fungiflora: Oslo, Norway, 2014; Volume 31, pp. 1-455.
10. Bernicchia, A.; Gorjón, S.P.; Arras, L.; Facchini, M.; Porcu, G.; Trichies, G. *Polypores of the Mediterranean region*; Romar: Segrate, Italy, 2020; pp. 904.
11. González, A.G.; Expósito, T.S.; Toledo Marante, F.J.; Pérez, M.J.M.; Tejera, E.B.; Bermejo Barrera, J. Lanosterol derivatives from *Phellinus torulosus. Phytochemistry* **1994**, *35*, 1523–1526.
12. Khadhri, A.; Aouadhi, C.; Aschi-Smiti, S. Screening of bioactive compounds of medicinal mushrooms collected on Tunisian territory. *Int. J. Med. Mushrooms* **2017**, *19*, 127–135.
13. Duru, M.E.; Tel-Çayan, G.; Deveci, E. Evaluation of phenolic profile, antioxidant and anticholinesterase effects of *Fuscoporia torulosa*. *Int. J. Second. Metab*. **2019**, 79–89.
14. Covino, S.; D'Ellena, E.; Tirillini, B.; Angeles, G.; Arcangeli, A.; Bistocchi, G.; Venanzoni, R.; Angelini, P. Characterization of biological activities of methanol extract of *Fuscoporia torulosa* (Basidiomycetes) from Italy. *Int. J. Med. Mushrooms* **2019**, *21*, 1051–1063.
15. Liu, H.-K.; Tsai, T.-H.; Chang, T.-T.; Chou, C.-J.; Lin, L.-C. Lanostane triterpenoids from the fungus *Phellinus gilvus*. *Phytochemistry* **2009**, *70*, 558–563.
16. González, A.G.; Expósito, T.S.; Toledo Marante, F.J.; Pérez, M.J.M.; Tejera, E.B.; Bermejo Barrera, J. Lanosterol derivatives from *Phellinus torulosus. Phytochemistry* **1994**, *35*, 1523–1526.
17. González, A.G.; Expósito, T.S.; Barrera, J.B.; Castellano, A.G.; Marante, F.J.T. The absolute stereochemistry of senexdiolic acid at C-22. *J. Nat. Prod.* **1993**, *56*, 2170–2174.
18. Kim, J.-P.; Yun, B.-S.; Shim, Y.K.; Yoo, I.-D. Inoscavin A, a new free radical scavenger from the mushroom *Inonotus xeranticus*. *Tetrahedron Lett.* **1999**, *40*, 6643–6644.
19. Bagno, A.; Rastrelli, F.; Saielli, G. Toward the complete prediction of the ^{1}H and ^{13}C NMR spectra of complex organic molecules by DFT methods: application to natural substances. *Chem. Eur. J.* **2006**, *12*, 5514–5525.
20. Barone, G.; Gomez-Paloma, L.; Duca, D.; Silvestri, A.; Riccio, R.; Bifulco, G. Structure validation of natural products by quantum-mechanical GIAO calculations of ^{13}C NMR chemical shifts. *Chemistry* **2002**, *8*, 3233–3239.
21. Grimblat, N.; Zanardi, M.M.; Sarotti, A.M. Beyond DP4: An improved probability for the stereochemical assignment of isomeric compounds using quantum chemical calculations of NMR shifts. *J. Org. Chem.* **2015**, *80*, 12526–12534.
22. Smith, S.G.; Goodman, J.M. Assigning stereochemistry to single diastereoisomers by GIAO NMR calculation: The DP4 probability. *J. Am. Chem. Soc.* **2010**, *132*, 12946–12959.
23. Bochevarov, A.D.; Harder, E.; Hughes, T.F.; Greenwood, J.R.; Braden, D.A.; Philipp, D.M.; Rinaldo, D.; Halls, M.D.; Zhang, J.; Friesner, R.A. Jaguar: A High-performance quantum chemistry software program with strengths in life and materials sciences. *Int. J. Quantum Chem.* **2013**, *113*, 2110–2142, doi:10.1002/qua.24481.
24. Chou, T.-C. Theoretical basis, experimental design, and computerized simulation of synergism and antagonism in drug combination studies. *Pharmacol. Rev.* **2006**, *58*, 621–681.
25. Chou, T.-C. Drug combination studies and their synergy quantification using the Chou-Talalay method. *Cancer Res.* **2010**, *70*, 440–446.

 doi:10.20944/preprints202102.0282.v1

26. Galip Akaydin, E.M.-S.; Sevgi Yardim-Akaydin, E.C.-C. Evalution of antioxidant activity of various herbal folk medicines. *J. Nutr. Food Sci.* **2013**, *3*, 222.
27. Mielnik, M.B.; Rzeszutek, A.; Triumf, E.C.; Egelandsdal, B. Antioxidant and other quality properties of reindeer muscle from two different Norwegian regions. *Meat Sci.* **2011**, *89*, 526–532.